J. Opt. A: Pure Appl. Opt. **2** (2000) 557–564. Printed in the UK PII: S1464-4258(00)13120-4

# Analytic propagation matrix method for anisotropic magneto-optic layered media

**I Abdulhalim**

Department of Electronics and Physics—Thin Films Centre, University of Paisley, Paisley PA1 2BE, Scotland, UK

Received 5 April 2000, in final form 30 August 2000

**Abstract.** Simplified analytic expressions are derived for the optical propagation matrix of magnetic anisotropic Kerr media using the Lagrange–Sylvester interpolation polynomial. This expression is used to investigate magnetic Kerr films in Fabry–Pérot configurations, magneto-optic recording quadrilayers and alternating periodic stacks. It is found that the magneto-optic reflection coefficients are enhanced by a few orders of magnitude due to multiple reflections. Bragg-type reflection peaks from periodic structure appear solely due to the gyrotropy and it is shown that omnidirectional reflection is possible under certain conditions. This analytic approach is faster than using direct numerical calculation.

**Keywords:** Multilayers, magneto-optics, omnidirectional reflectors, periodic media, thin films

## 1. Introduction

Media with anti-symmetric dielectric tensors occur in Nature due to time and space invariance such as with optically active chiral media and Faraday rotation in magnetic Kerr media respectively [1]. Following Faraday's discovery [1, 2], Kerr found that light reflected from magnetized iron changes its polarization state upon reflection with dependence on the magnetic field. These media find applications in a wide variety of situations including optical data storage, sensors, isolators and modulators [2]. Their optical properties were investigated extensively in the last decade due to their potential modern applications [3–20]. The optics of slabs and hence multilayers were treated with numerical calculations using methods such as the $2 \times 2$ [13] or $4 \times 4$ matrix approaches [3,9,20–24]. The $4 \times 4$ matrix approach [21–24], in particular, as formulated by Berreman [21], is the most sensible way to solve such problems because of its simple implementation. This approach involves calculation of the eigenvalues and the exponents of $4 \times 4$ matrices to find the propagation matrix of the slab. De Smet [3] has used this approach to find analytic expressions for the Fresnel reflection coefficients from isotropic polar Kerr media at their interface with isotropic medium. The exponent of the $4 \times 4$ matrix defines a $4 \times 4$ propagation matrix from which all the linear optical properties of the layer can be deduced. To simplify this calculation, the use of the Lagrange–Sylvester interpolation polynomial [25] was proposed originally by Abdulhalim *et al* [26, 27] and later used in the Cayley–Hamilton form by Wohler *et al* [28]. Recently [29], we generalized this calculation to an arbitrary biaxial medium and presented in brief the simplified $4 \times 4$ propagation matrix for some special cases. In this paper, we present in detail for the first time a simplified expression for the propagation matrix of a slab of a magneto-optic layer and apply it to polar, longitudinal and transverse Kerr multilayered structures. Numerical simulations are presented for a magneto-optic quadrilayer stack used in optical data storage, for Kerr media in the Fabry–Pérot configuration and for a periodic stack of alternating Kerr and dielectric layers. In section 2 the formulation of the problem is presented and in section 3 we present numerical results.

## 2. Formulation

The problem under consideration involves a biaxial magneto-optic medium with oblique magnetization where the magnetization vector makes an angle $\Theta$ with the $Z$-axis (polar angle) and its projection on the $XY$-plane makes the azimuth $\Phi$ with the $X$-axis (figure 1). The dielectric tensor has the following anti-symmetric form:

$$\bar{\varepsilon} = \begin{pmatrix} \varepsilon_{xx} & \cos\Theta\varepsilon'_{xy} & -\sin\Theta\sin\Phi\varepsilon'_{xy} \\ -\cos\Theta\varepsilon'_{xy} & \varepsilon_{yy} & \sin\Theta\cos\Phi\varepsilon'_{xy} \\ \sin\Theta\sin\Phi\varepsilon'_{xy} & -\sin\Theta\cos\Phi\varepsilon'_{xy} & \varepsilon_{zz} \end{pmatrix} \quad (1)$$

where $\varepsilon_{xx} = \varepsilon_1$, $\varepsilon_{yy} = \varepsilon_2$ and $\varepsilon_{zz} = \varepsilon_3$ could be complex and $\varepsilon'_{xy} = -\mathrm{i}g$, where $g$ defines the gyrotropy factor responsible for the magneto-optic effect and in first approximation linear with the magnetization vector. From equation (1) three cases are distinguished: (1) the polar Kerr effect ($\Theta$, $\Phi = 0$), (2) longitudinal Kerr effect ($\Theta = \pi/2$, $\Phi = 0$) and (3) transverse Kerr effect ($\Theta$, $\Phi = \pi/2$). For an isotropic medium, the magnetization induces uniaxial anisotropy [3], $\varepsilon_3 \neq \varepsilon_1 = \varepsilon_2$, which is usually neglected; however, we shall present the

1464-4258/00/060557+08$30.00  

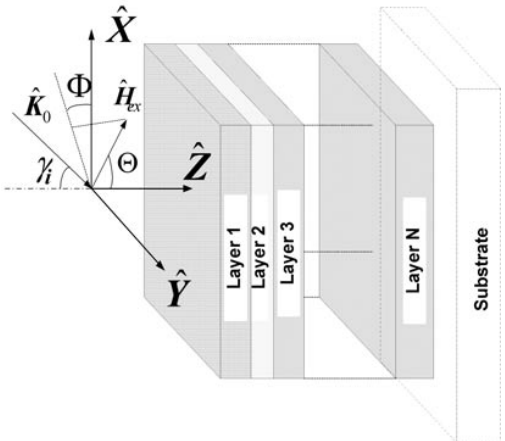


**Figure 1.** Schematic drawing of the geometry of a general multilayered stack involving magneto-optic layers. The external magnetic field is applied obliquely and the light is incident from a semi-infinite isotropic medium.

solution to the general anisotropic case $\varepsilon_3 \neq \varepsilon_1 \neq \varepsilon_2$ as well. The dielectric tensor elements have a dispersion form similar to a harmonic oscillator dispersion since their derivation is stimulated from the response of an electron bound by a harmonic potential and subject to a static magnetic field [3]. The electromagnetic wave is taken to be incident on the multilayered medium from an isotropic semi-infinite medium at an angle of incidence $\gamma_i$ with respect to the $Z$-axis and without loss of generality we take the incidence plane as the $XZ$-plane (see figure 1).

Within the $4 \times 4$ matrix approach the electric and magnetic field components of $\vec{E}(z)\exp(\mathrm{i}k_z z)$ and $\vec{H}(z)\exp(\mathrm{i}k_z z)$ are arranged in a column form: $\Psi = (\sqrt{\varepsilon_0}E_x, \sqrt{\mu_0}H_y, \sqrt{\varepsilon_0}E_y, -\sqrt{\mu_0}H_x)^{\mathrm{T}}\exp(\mathrm{i}k_z z)$, with $\varepsilon_0$ and $\mu_0$ being the permittivity and permeability of free space respectively. Maxwell's equations may then be written in the form of a first-order system of differential equations:

$$\frac{\partial \Psi}{\partial z} = \mathrm{i}k_0 \Delta \Psi \tag{2}$$

where the matrix $\Delta$ is given by

$$\Delta = \begin{pmatrix} -\nu_x\varepsilon_{zx}/\varepsilon_{zz} & 1-\nu_x^2/\varepsilon_{zz} & -\nu_x\varepsilon_{zy}/\varepsilon_{zz} & 0 \\ \varepsilon_{xx}-\varepsilon_{xz}\varepsilon_{zx}/\varepsilon_{zz} & -\nu_x\varepsilon_{xz}/\varepsilon_{zz} & \varepsilon_{xy}-\varepsilon_{xz}\varepsilon_{zy}/\varepsilon_{zz} & 0 \\ 0 & 0 & 0 & 1 \\ \varepsilon_{yx}-\varepsilon_{yz}\varepsilon_{zx}/\varepsilon_{zz} & -\nu_x\varepsilon_{yz}/\varepsilon_{zz} & \varepsilon_{yy}-\nu_x^2-\varepsilon_{yz}\varepsilon_{zy}/\varepsilon_{zz} & 0 \end{pmatrix} \tag{3}$$

and the indices $\nu_x$ and $\nu_z$ define the direction cosines of the $\vec{k}$-vector: $\vec{k} = k_0(\nu_x, 0, \nu_z)$, where $k_0 = 2\pi/\lambda_0$, is the propagation wavenumber in free space.

We consider the three main cases of magnetization orientations: polar, longitudinal and transverse. Here we present a detailed description for the polar Kerr effect while for the other two cases the main results are summarized in the appendix. The elements of the $\Delta$-matrix for the polar Kerr case are given by

$$\Delta = \begin{pmatrix} 0 & 1-\nu_x^2/\varepsilon_{zz} & 0 & 0 \\ \varepsilon_{xx} & 0 & \varepsilon_{xy} & 0 \\ 0 & 0 & 0 & 1 \\ \varepsilon_{yx} & 0 & \varepsilon_{yy}-\nu_x^2 & 0 \end{pmatrix}. \tag{4}$$

The general solution to equation (2) for a homogeneous medium is expressed as

$$\Psi(z) = \exp(\mathrm{i}k_0\Delta z)\Psi(0). \tag{5}$$

In order to simplify the calculation of the exponent of the $4 \times 4$ matrix we have to find its eigenvalues first. These can be shown to be the eigenindices of the characteristic waves since within a homogeneous region $\partial_z\Psi = \mathrm{i}k_z\Psi$, which, when inserted in equation (2), leads to the secular equation $|\Delta - \nu_z| = 0$, that has the following roots:

$$\nu_z = \pm\sqrt{\frac{\Delta_{12}\Delta_{21} + \Delta_{43} \pm \sqrt{(\Delta_{12}\Delta_{21}-\Delta_{43})^2 + 4\Delta_{12}\Delta_{41}\Delta_{23}}}{2}}. \tag{6}$$

Discussion on the nature of the eigenwaves can be found in [29]. Now that the eigenvalues of the $\Delta$-matrix are found, we can calculate any function of it using the Lagrange–Sylvester interpolation theorem [25], assuming all of its eigenvalues are distinct. For the procedure of this calculation as well as for the case of degenerate eigenmodes (such as for an isotropic layer) the reader is referred to [29].

Assuming a slab of thickness $h$ bounded between two semi-infinite media, the matrix $P(h) = \exp(\mathrm{i}k_0 h\Delta)$ relates the field components at $z = h$ to those at 0, which is known as the propagation matrix or the propagator. Its inverse $M(h) = \exp(-\mathrm{i}k_0 h\Delta)$ is known traditionally as the characteristic matrix. The reflection and transmission coefficients could then be expressed in terms of the elements of these matrices. Since the eigenindices are known and they come in pairs, that is, $\nu_{z1} = -\nu_{z3}$ and $\nu_{z2} = -\nu_{z4}$, the propagation matrix could be reduced to a simple analytic form. The matrix $P(h)$ then takes the following form:

$$P = \begin{pmatrix} -f_2 - \Delta_{12}\Delta_{21}f_3 & \Delta_{12}^2\Delta_{21}f_1 + \Delta_{12}f_4 & -\Delta_{12}\Delta_{23}f_3 & \Delta_{12}\Delta_{23}f_1 \\ b_1 f_1 + \Delta_{21}f_4 & P_{11} & -b_2\Delta_{23}f_1 + \Delta_{23}f_4 & -\Delta_{23}f_3 \\ -P_{24} & -P_{14} & -f_2 - \Delta_{43}f_3 & \Delta_{43}f_1 + f_4 \\ -P_{23} & -P_{13} & b_3 f_1 + \Delta_{43}f_4 & P_{33} \end{pmatrix} \tag{7}$$

where $b_1 = \Delta_{21}^2\Delta_{12} - \Delta_{23}^2$, $b_2 = -(\Delta_{43} + \Delta_{12}\Delta_{21})$, $b_3 = \Delta_{43}^2 - \Delta_{12}\Delta_{23}^2$ and

$$\begin{aligned} f_1 &= -\mathrm{i}\frac{\nu_{z1}\sin(k_0 h\nu_{z2}) - \nu_{z2}\sin(k_0 h\nu_{z1})}{\nu_{z1}^3\nu_{z2} - \nu_{z2}^3\nu_{z1}} \\ f_2 &= \frac{\nu_{z2}^2\cos(k_0 h\nu_{z1}) - \nu_{z1}^2\cos(k_0 h\nu_{z2})}{\nu_{z1}^2 - \nu_{z2}^2} \\ f_3 &= \frac{\cos(k_0 h\nu_{z2}) - \cos(k_0 h\nu_{z1})}{\nu_{z1}^2 - \nu_{z2}^2} \\ f_4 &= \mathrm{i}\frac{\nu_{z1}^3\sin(k_0 h\nu_{z2}) - \nu_{z2}^3\sin(k_0 h\nu_{z1})}{\nu_{z1}^3\nu_{z2} - \nu_{z2}^3\nu_{z1}}. \end{aligned} \tag{8}$$

Note that only ten of the 16 elements of the matrix $P$ are required. The characteristic matrix $M$ is given by the same expressions upon substituting $h \to -h$, which gives the same form of the matrix $P$ with $f_1 \to -f_1$ and $f_4 \to -f_4$.

In certain special cases equation (7) could be reduced to simpler forms: for example, for the isotropic case we have $\Delta_{12}\Delta_{21} = \Delta_{43}$, which gives all the diagonal elements equal to $P_{11}$. For the uniaxial case at normal incidence we have $\Delta_{12} = 1$ and $\Delta_{21} = \Delta_{43}$; the matrix $P$ becomes

$$P = \begin{pmatrix} -f_2 - \Delta_{21}f_3 & \Delta_{21}f_1 + f_4 & -\Delta_{23}f_3 & \Delta_{23}f_1 \\ b_1 f_1 + \Delta_{21}f_4 & P_{11} & 2\Delta_{21}\Delta_{23}f_1 + \Delta_{23}f_4 & -P_{13} \\ P_{13} & -P_{14} & P_{11} & P_{12} \\ -P_{23} & -P_{13} & P_{21} & P_{11} \end{pmatrix} \tag{9}$$

showing that only six elements are required in this case. The uniaxial case simulates what is called cold magneto-plasma such as the case of magnetic field induced gyrotropy in free-carrier systems existing for example in semiconductors, metals or the ionosphere [1, 2, 20].

For a multilayered structure with $N$ layers, stacked from top to bottom in the order $j = 1, 2, 3, \ldots, N-1, N$, assuming each layer $j$ is characterized by its own propagator $P_j$ or characteristic matrix $M_j$, then the total matrix characterizing the structure is given by the matrix product:

$$P = P_N P_{N-1}, \ldots, P_{j+1} P_j P_{j-1}, \ldots, P_1$$
$$M = \prod_{j=1}^{N} M_j. \tag{10}$$

Here we should mention that, for isotropic layers that could be part of the stack, the eigenindices are degenerate and the Lagrange–Sylvester and Cayley–Hamilton theorems [25] are not valid and exhibit singularity. To avoid this we used [29] what is called the fundamental theorem from matrix algebra and obtained a simplified expression for a dielectric isotropic layer.

The reflection and transmission coefficients are then expressed [29] in terms of the elements of the propagation matrix by matching the tangential field components at the external boundaries. This assumes the light is incident at an angle $\gamma_i$, from a semi-infinite isotropic medium with refractive index $n_i$, and transmitted to a second semi-infinite isotropic medium with corresponding angle and refractive index $\gamma_t$ and $n_t$, respectively. When the matrix $P$ is block diagonal the reflection and transmission matrices become diagonal, meaning that the two modes are the TE and TM modes, which are not coupled. This is the case for the transverse Kerr effect (appendix) where the magnetization affects only the intensity of the reflected light, not its polarization.

## 3. Numerical results

The analytic expressions derived for the propagation matrices have been applied to calculate the optical properties of a number of multilayered structures as presented in the following subsections. The calculations were performed using Mathematica 3.0 software.

### 3.1. Optical recording quadrilayer

Multilayer magneto-optic recording media are based on the fact that the optical interference of the multilayered medium enhances the reflectivity component induced by the polar Kerr effect in the magnetic layer and, therefore, increases the signal-to-noise ratio. The recording medium consists of four layers on a substrate: the overcoat, which acts both as an antireflection layer and a protection layer; the magnetic layer, which causes the polar Kerr effect; an intermediate phase matching layer and finally a reflectance layer.

In order to check the correctness of the expressions derived and demonstrate our approach, we consider the quadrilayer structure used by Balasubramanian *et al* [19] and by Mansuripur [13]. It consists of a glass substrate

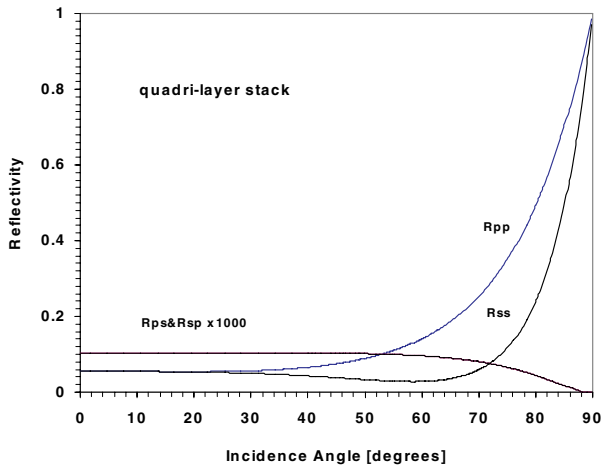


**Figure 2.** The reflectivity coefficients as a function of the incidence angle for a quadrilayer typical for magneto-optic recording medium (see text for the parameters used). Note that $R_{ps} = R_{sp}$.
(This figure is in colour only in the electronic version, see `www.iop.org`)

with refractive index $n_{sub} = 1.5$, coated with a reflecting aluminum layer of thickness 500 nm and complex refractive index $n_{Al} = 2.75 + 8.31i$. A quarter-wave layer of $SiO_x$ (143.2 nm thick), with $n_{SiO_x} = 1.449$, separates the aluminum layer from the magnetic film, which is 20 nm thick and has the following nonzero elements of the dielectric tensor: $\varepsilon_{xx} = \varepsilon_{yy} = \varepsilon_{zz} = -4.8984 + 19.415i$ and $\varepsilon_{xy} = -\varepsilon_{yx} = 0.4322 + 0.0058i$. The overcoat layer is another quarter-wave $SiO_x$ layer and the light is incident from air with a wavelength of $\lambda_0 = 830$ nm. The propagation matrix for this quadrilayer is given by

$$P_{quad} = P_{Al} P_{SiO_x} P_{MO} P_{SiO_x} \tag{11}$$

where here $P_{Al}$ and $P_{SiO_x}$ correspond to the isotropic Al and $SiO_x$ layers respectively [29], while $P_{MO}$ represents the magneto-optic layer of the form presented in equation (7). Results of the calculated reflectivities are presented in figure 2. The results are in full agreement with the previously reported results [13, 19]. Note that, in figure 2, we present the reflectivity itself rather than its amplitude as presented in [13]. Note that a Brewster-type angle appears in $R_{ss}$ but not in $R_{pp}$. This is unique for this special multilayer system and not for any isotropic Kerr medium interface as will be shown later. We should note here that the CPU time required (using a 100 MHz processor) to calculate figure 2 was 56 s while using direct numerical calculation it took 97 s. Hence we conclude that this method is faster by nearly a factor of two.

### 3.2. Multiple-reflection enhancement of the Kerr effect

In the magnetic Kerr effect the rotation of the plane of polarization does not depend on whether the light propagates in the same direction as the magnetization vector or opposite to it, a fact which forms the basis for Faraday isolators. Hence, upon multiple reflections, the polarization rotation is expected to be enhanced, and the Fabry–Pérot configuration can yield a large magneto-optic effect. To demonstrate this

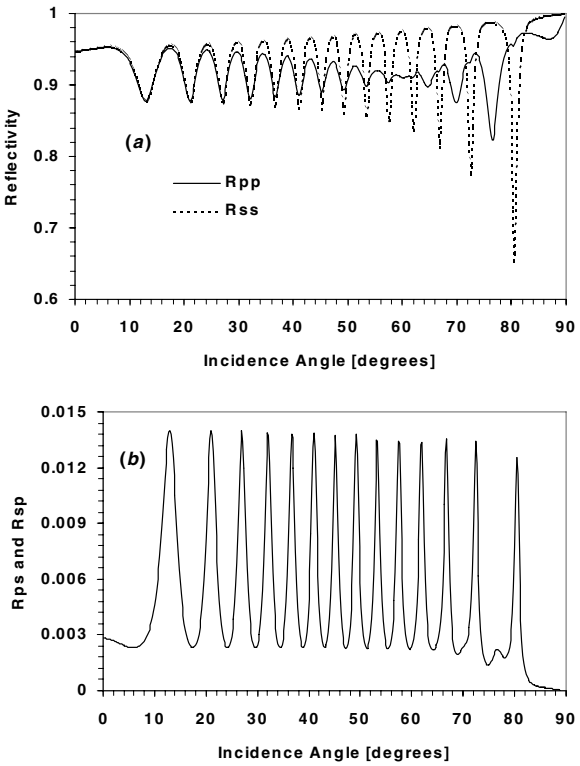


**Figure 3.** Reflectivity from magneto-optic polar Kerr film deposited on a silver substrate.

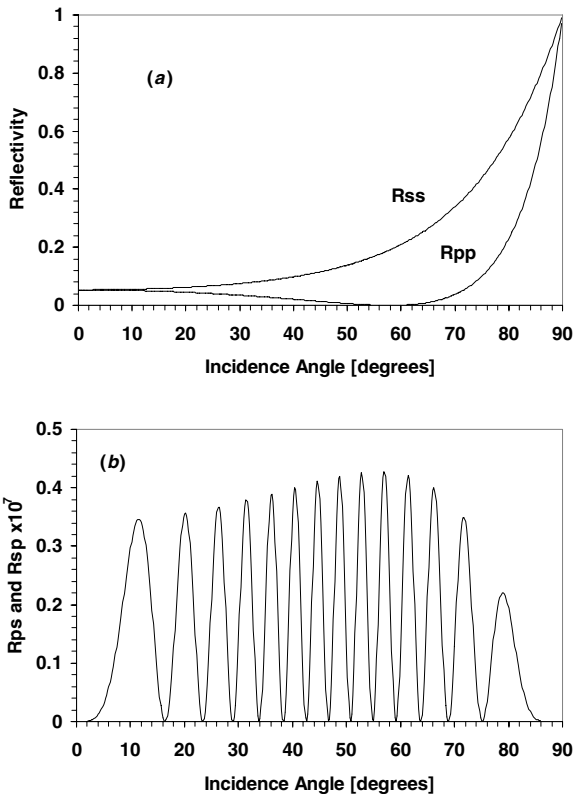


**Figure 4.** Reflectivity from the same magneto-optic polar Kerr film of figure 3 but deposited on an index matched substrate ($n_{\text{sub}} = 1.6$). Comparison with figure 3 shows the strong enhancement of the magneto-optic reflection coefficients due to multiple reflections.

effect we considered a magnetic film with thickness equal to 20 wavelengths deposited on silver substrate in one case and on an index matching substrate in another case. For the polar Kerr configuration the following nonzero elements of the dielectric tensor were taken: $\varepsilon_{xx} = \varepsilon_{yy} = \varepsilon_{zz} = 2.56$, $\varepsilon_{xy} = -\varepsilon_{yx} = 0.001\text{i}$, and the index for silver is $n_{\text{sub}} = 0.18 + 3.64\text{i}$. In figures 3 and 4 we present the results of this calculation, showing that for the silver substrate case (figure 3) the magneto-optic effect is enhanced by six orders of magnitude due to multiple reflections. This fact could be used to simplify the measurement of Kerr coefficients for magneto-optic thin films and for building highly efficient magneto-optic devices.

### 3.3. Periodic stack

The structure of an alternating stack of layers known as a Bragg reflector has been studied extensively in the literature [30] for the case of isotropic dielectric layers. Here we consider this structure where one of the alternating layers is a magneto-optic layer while the other layer is dielectric. The propagation matrix for one period of the structure is

$$P_{\text{per}} = P_{\text{diel}} P_{\text{MO}} \tag{12}$$

where $P_{\text{MO}}$ and $P_{\text{diel}}$ are the propagation matrices for the magneto-optic and dielectric layers of thicknesses $h_1$ and $h_2$ respectively. If the number of periods is $N_{\text{p}}$, then the total propagation matrix is $(P_{\text{diel}})^{N_{\text{p}}}$. Since the magneto-optic matrix $P_{\text{MO}}$ is not block diagonal, the total propagation matrix will not be block diagonal, meaning that there is coupling between the TE and TM waves. For an infinite structure the eigenwaves are Bloch–Floquet type waves, which are plane waves modulated by a function periodic with the structure and their wavevectors being determined by the following dispersion relation:

$$|P_{\text{per}} - \exp(\text{i}kh)| = 0 \tag{13}$$

where $h = h_1 + h_2$ is the period. The four solutions to this equation yield the wavevectors for the system normal modes and each eigenwave is an eigenvector of $P_{\text{per}}$. Two of the solutions represent forward propagating waves (positive group velocity) and the other two are backward propagating (negative group velocity) created at the second boundary. The wavevectors are usually complex with their real part versus the wavelength representing the dispersion curve while the positive imaginary part represents the attenuation factor of a Bragg reflected wave. Bragg reflections occur when either one of the following conditions is satisfied:

$$k_{1,2}h = n\pi, \qquad \text{or} \qquad k_1 h + k_2 h = m\pi, \tag{14}$$

where $n, m = 0, \pm 1, \pm 2, \ldots$.

The first condition defines the resonant Bragg reflection and does not involve polarization conversion; it is a direct consequence of coupling between the forward and backward propagating waves of the same type. The diagonal elements of the dielectric tensor are responsible for this type of

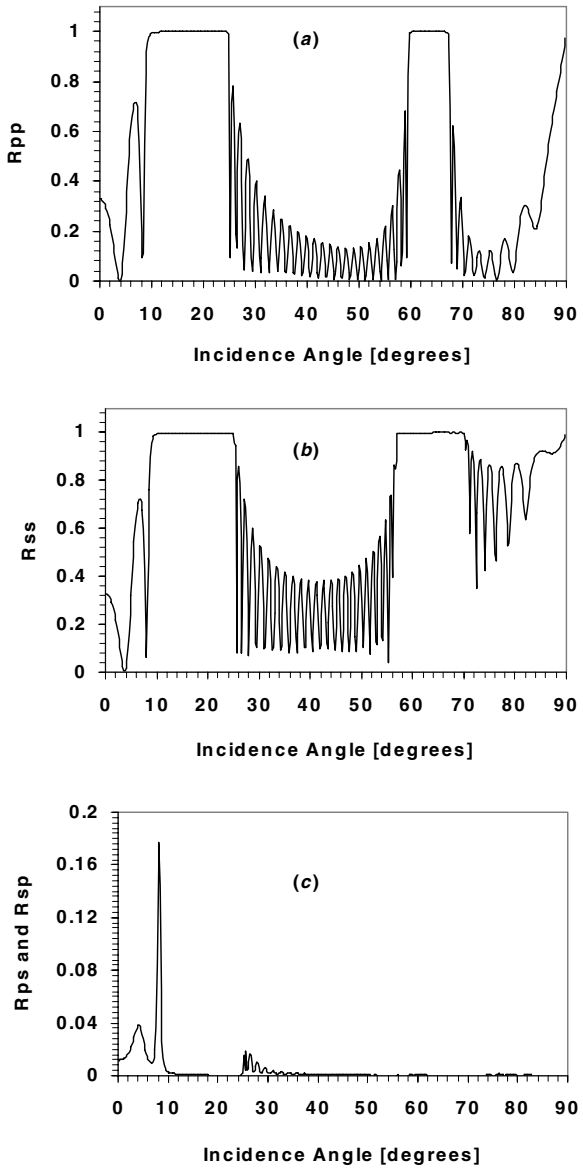


**Figure 5.** Reflection coefficients from an alternating stack of magneto-optic and dielectric films. See the text for the parameters used.

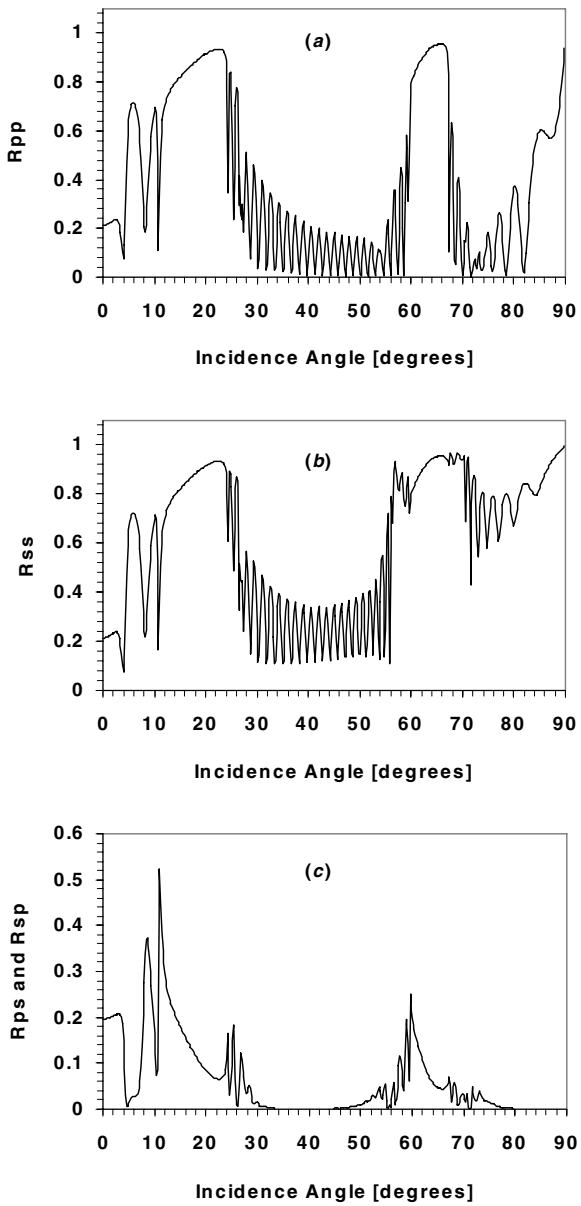


**Figure 6.** Reflection coefficients from the same structure as figure 5 but with a larger gyrotropy, showing the enhancement of the polarization conversion peaks.

reflection. The second condition is the exchange Bragg reflection, that yields a different type of reflection where polarization conversion occurs. It is the result of the off-diagonal elements of the dielectric tensor that cause the coupling between modes of different types. For a detailed discussion on these types of reflection the reader is referred to [27, 30, 36].

Figure 5 shows the reflectivity curves for an alternating layers of a magneto-optic film and dielectric layer. The magneto-optic layer has the same parameters as that in figures 3 and 4 except that its thickness is $h_1 = 2\lambda_0$, while the dielectric layer has an index of refraction of 2.5 and thickness $h_2 = 0.15\lambda_0$. The whole structure is deposited on a substrate with refractive index of 1.55 and the number of periods is $N_p = 25$. Two main resonant Bragg reflection peaks appear in $R_{pp}$ and $R_{ss}$ while a series of exchange peaks appears in $R_{ps} = R_{sp}$ with decaying height. The exchange peaks appear solely due to the off-diagonal elements of the dielectric tensor, or in other words due to the gyrotropic coefficient. Note that the first peak could be easily measured, hence it yields another way for enhancing the magneto-optic effect. In order to observe the behaviour of all the exchange peaks we increased the off-diagonal element of the magneto-optic dielectric tensor to $\varepsilon_{xy} = -\varepsilon_{yx} = 0.015\mathrm{i}$. The result is shown in figure 6, which shows that the exchange peaks exhibit a fine structure more likely composed of triplets and they shift, widen and increase in height with the gyrotropy. Because the peaks now are more pronounced and some of them fall in the same region as the resonant peaks, they influence the shape of the resonant peaks. In order to clarify whether the structure of

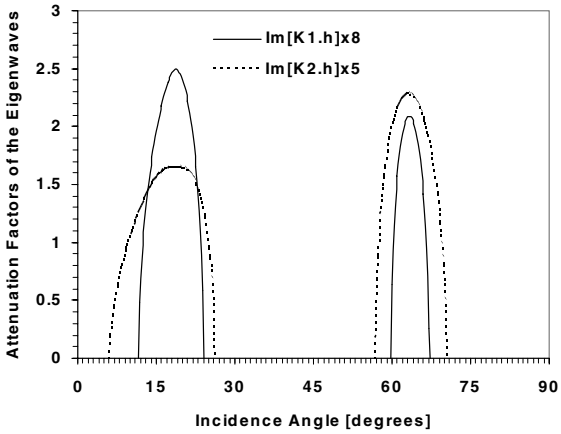


**Figure 7.** The attenuation factors versus the incidence angle for the same structure as figure 6.

the exchange peaks originates from multiple reflections we performed a calculation of the dispersion curves. Figure 7 shows the imaginary parts of the products $k_{1,2}h$ known as the attenuation factors. One can see that the attenuation factor for mode 1 has a more symmetric shape than that for mode 2 and it is narrower. Hence when compared to figure 6 we can conclude that mode 1 is nearly p polarized while mode 2 is nearly s polarized. According to figure 7 there is no splitting of the attenuation factors; however, their asymmetry perhaps originates from the existence of some fine structure. The asymmetry of $k_{1,2}h$ is larger for the higher-order reflection peak (smaller angles). This may be associated with the stronger appearance of the exchange peaks corresponding to the same Bragg angle. For the longitudinal Kerr media, figure 8 shows that the order of appearance of the exchange peaks is reversed; however, they exhibit similar fine structure and their height is smaller as compared to those in figure 5. The resonant Bragg peaks of $R_{pp}$ and $R_{ss}$ for the polar (figures 5($a$) and ($b$)) and longitudinal (figures 8($a$) and ($b$)) cases are identical, as expected, because the diagonal elements of the dielectric tensor are basically identical.

Apart from Bragg reflections, an alternating periodic two-layer system has been shown recently [31–35] to exhibit a photonic band gap behaviour. Under certain conditions the structure exhibits omnidirectional reflection in a wide spectral range. This was demonstrated both theoretically and experimentally in the infra-red and visible spectral ranges. Recently [36], we have shown that this omnidirectional reflection is also possible with alternating anisotropic layers similar to a Solc filter structure. Here we consider the possibility of an omnidirectional reflector using the same periodic system as used in figure 5 except that $h_1 = h_2$ and $N_p = 20$. Figures 9 and 10 show $R_{pp}$ and $R_{ss}$ curves for three different values of the period: $h = 0.22\lambda_0$, $0.26\lambda_0$ and $0.28\lambda_0$, where the omnidirectional reflection occurs at $h = 0.26\lambda_0$. The change in $h$ required to open a pass-band is smaller for $R_{pp}$ (only $0.004\lambda_0$) than for $R_{ss}$ (nearly $0.008\lambda_0$) because of the existence of Brewster's angle in $R_{pp}$. Here we should mention that the omnidirectional reflection in $R_{pp}$ and $R_{ss}$ curves is not complete because of some reflectivity in $R_{ps}$ and $R_{sp}$; however, it is smaller

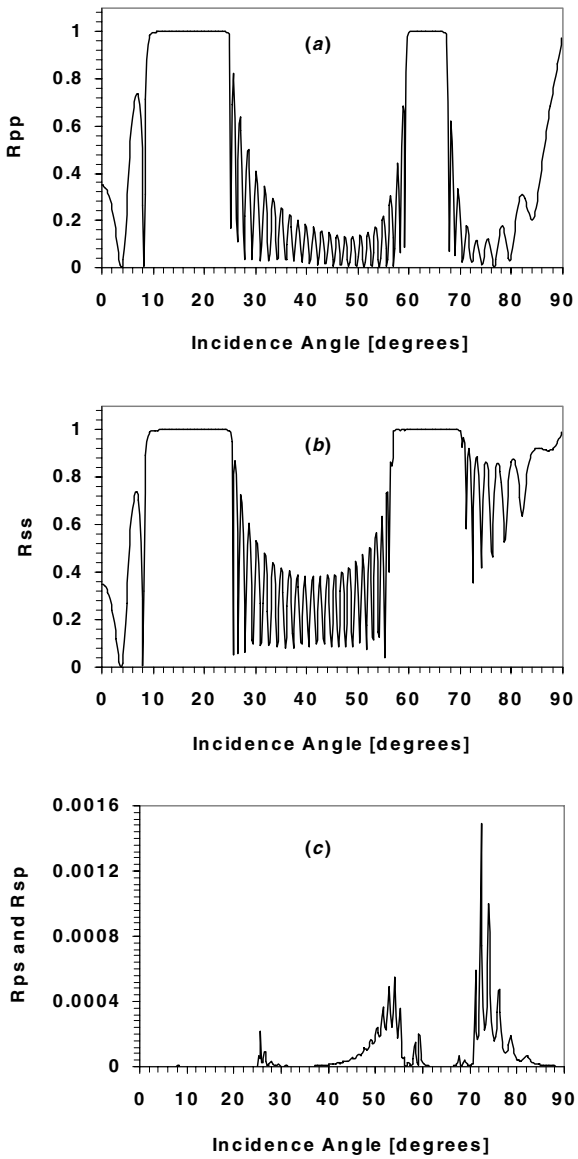


**Figure 8.** Reflection coefficients from an alternating stack of magneto-optic and dielectric films with the same parameters as in figure 5 except that we used the longitudinal Kerr magneto-optic effect instead of the polar Kerr.

by a few orders of magnitude and therefore negligible and not shown here. However, in a similar manner to what was observed in [36], the total reflection coefficients, that is $R_{tp} = R_{pp} + R_{ps}$ and $R_{ts} = R_{ss} + R_{sp}$, exhibit the full omnidirectional behaviour. Nevertheless figures 9 and 10 show that it is possible to use magneto-optic materials in periodic stacks that exhibit omnidirectional reflection.

## 4. Conclusions

The optical properties of magneto-optic media incorporated in Fabry–Pérot configuration and multilayers were investigated using a simplified analytic $4 \times 4$ matrix method. Simplified algebraic expressions were derived for the single-layer propagation matrix of magneto-optic layers in the

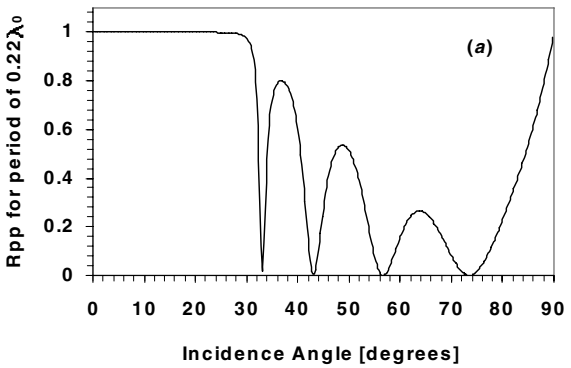


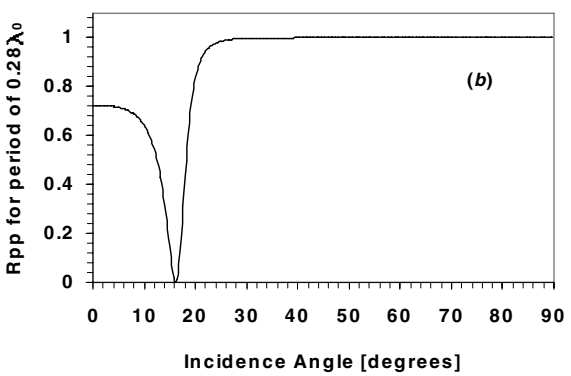


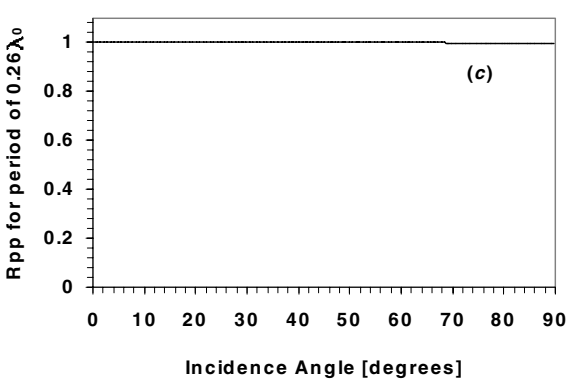


**Figure 9.** Reflection coefficient for p-polarized light from the same structure as in figure 5 except that the layer thicknesses are different. This shows that in certain conditions the structure exhibits omnidirectional reflection. See the text for the other parameters.

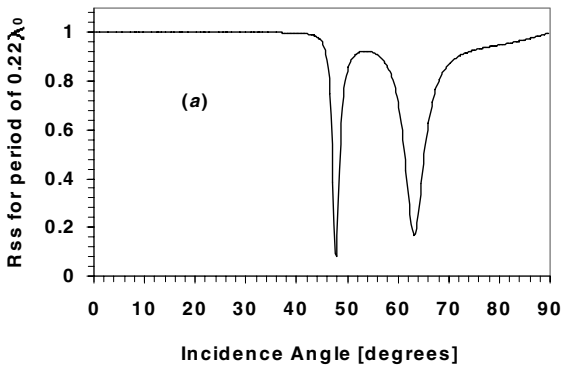


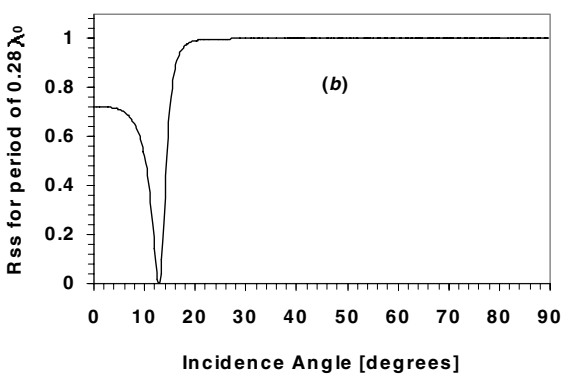


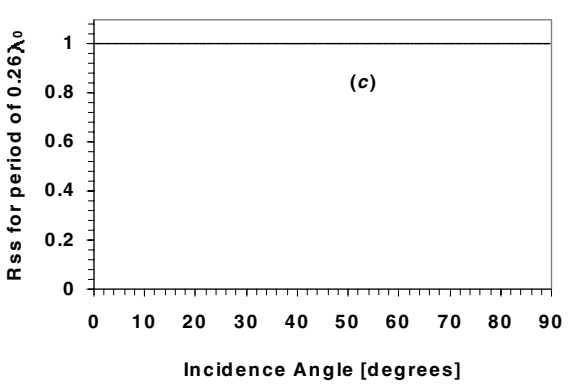


**Figure 10.** Reflection coefficient for s-polarized light from the same structure as in figure 5 except that the layer thicknesses are different. This shows that in certain conditions the structure exhibits omnidirectional reflection. See the text for the other parameters.

polar, longitudinal and transverse configurations. It was shown that this approach allows a faster speed of calculation by a factor of two. The magneto-optic reflection coefficients were shown to be enhanced by a few orders of magnitude in the Fabry–Pérot configuration due to multiple reflections and Bragg-type reflection peaks from periodic structure appear solely due to the gyrotropy. We showed also that omnidirectional reflection from a periodic stack that contains magneto-optic layers is possible under certain conditions. The analytic simplified expressions derived in this paper are useful for the analysis of data from magneto-optic structures and for the design of devices.

## Appendix. Longitudinal and transverse Kerr media

The $\Delta$-matrix for the longitudinal Kerr media is given by

$$\Delta = \begin{pmatrix} 0 & 1-\nu_x^2/\varepsilon_{zz} & -\nu_x\varepsilon_{zy}/\varepsilon_{zz} & 0 \\ \varepsilon_{xx} & 0 & 0 & 0 \\ 0 & 0 & 0 & 1 \\ 0 & -\nu_x\varepsilon_{yz}/\varepsilon_{zz} & \varepsilon_{yy}-\nu_x^2-\varepsilon_{yz}\varepsilon_{zy}/\varepsilon_{zz} & 0 \end{pmatrix} \tag{A1}$$

where $\varepsilon_{yz} = -\mathrm{i}g = -\varepsilon_{zy}$. The eigenindices are given by

$$\nu_z = \pm\sqrt{\frac{\Delta_{12}\Delta_{21} + \Delta_{43} \pm \sqrt{(\Delta_{12}\Delta_{21}-\Delta_{43})^2 - 4\Delta_{13}^2\Delta_{21}}}{2}}. \tag{A2}$$

The single-layer propagation matrix is then

$$P = \begin{pmatrix} -f_2 - \Delta_{12}\Delta_{21} f_3 & c_1 f_1 + \Delta_{12} f_4 & -c_2\Delta_{13} f_1 + \Delta_{13} f_4 & -\Delta_{13} f_3 \\ c_3 f_1 + \Delta_{21} f_4 & P_{11} & -\Delta_{21}\Delta_{13} f_3 & \Delta_{21}\Delta_{13} f_1 \\ -P_{24} & -P_{14} & -f_2 - \Delta_{43} f_3 & \Delta_{43} f_1 + f_4 \\ -P_{23} & -P_{13} & c_4 f_1 + \Delta_{43} f_4 & P_{33} \end{pmatrix} \tag{A3}$$

where $c_1 = \Delta_{12}^2\Delta_{21} - \Delta_{13}^2$, $c_2 = -(\Delta_{43} + \Delta_{12}\Delta_{21})$, $c_3 = \Delta_{12}\Delta_{21}^2 - \Delta_{13}^2$ and $c_4 = \Delta_{43}^2 - \Delta_{21}\Delta_{13}^2$.

For the transverse Kerr effect the $\Delta$-matrix is given by

$$\Delta = \begin{pmatrix} -\nu_x\varepsilon_{zx}/\varepsilon_{zz} & 1 - \nu_x^2/\varepsilon_{zz} & 0 & 0 \\ \varepsilon_{xx} - \varepsilon_{xz}\varepsilon_{zx}/\varepsilon_{zz} & -\nu_x\varepsilon_{xz}/\varepsilon_{zz} & 0 & 0 \\ 0 & 0 & 0 & 1 \\ 0 & 0 & \varepsilon_{yy} - \nu_x^2 & 0 \end{pmatrix} \tag{A4}$$

where $\varepsilon_{xz} = \mathrm{i}g = -\varepsilon_{zx}$. The eigenindices are

$$\begin{aligned} \nu_{z1,3} &= \pm\sqrt{\Delta_{12}\Delta_{21} + \Delta_{11}^2} \\ \nu_{z2,4} &= \pm\sqrt{\Delta_{43}}. \end{aligned} \tag{A5}$$

To find the single-layer propagation matrix for this case we use the theorem [25], which states that any function of a block-diagonal matrix is a block-diagonal matrix with its blocks built by applying the same function to the constituent blocks. Hence for this case the problem is reduced to algebraic operations on $2 \times 2$ matrices. The net result is the following:

$$P = \begin{pmatrix} \mathrm{i}\Delta_{11}\sin(k_0 h\nu_{z1})/\nu_{z1} + \cos(k_0 h\nu_{z1}) & \mathrm{i}\Delta_{12}\sin(k_0 h\nu_{z1})/\nu_{z1} & 0 & 0 \\ \mathrm{i}\Delta_{21}\sin(k_0 h\nu_{z1})/\nu_{z1} & P_{11}^* & 0 & 0 \\ 0 & 0 & \cos(k_0 h\nu_{z2}) & \mathrm{i}\sin(k_0 h\nu_{z2})/\nu_{z2} \\ 0 & 0 & \mathrm{i}\nu_{z2}\sin(k_0 h\nu_{z2}) & P_{33} \end{pmatrix}. \tag{A6}$$

Note that since the $P$-matrix is block diagonal, in this case the two excited modes are the TE and TM modes and are not coupled, that is contrary to the other two cases; here we have $R_{ps} = R_{sp} = 0$. This is not surprising however, since in the transverse case there is no component of the applied magnetic field in the direction of propagation.

## References


[1] Landau L D and Lifshitz E M 1960 *Electrodynamics of Continuous Media* (New York: Pergamon)

[2] Mansuripur M 1995 *The Physical Principles of Magneto-Optical Recording* (Cambridge: Cambridge University Press)

[3] De Smet D J 1992 *J. Mod. Opt.* **39** 1055–65

[4] Elman J F, Greener J, Herzinger C M and Johs B 1998 *Thin Solid Films* **313/314** 816–20

[5] McGahan W A, He P and Woollam J A 1992 *Appl. Phys. Commun.* **11** 375–401

[6] McGahan W A and Woollam J A 1989 *Appl. Phys. Commun.* **9** 1–25

[7] Wierman K W, Hilfiker J N, Sabiryanov R F, Jaswal S S, Kirby R D and Woollam J A 1997 *Phys. Rev.* B **55** 3093–9

[8] Li Z-M and Parson R R 1988 *J. Opt. Soc. Am.* A **5** 1543–8

[9] Li Z-M, Sullivan B T and Parson R R 1988 *Appl. Opt.* **27** 1334–8

[10] Gamble R and Lissberger P H 1988 *J. Opt. Soc. Am.* A **5** 1533–42

[11] Barisov S B, Dadoenkova N N and Lyubchanskii I L 1993 *Opt. Spectrosc.* **74** 670–82

[12] Visnovsky S 1986 *Czech. J. Phys.* B **36** 625–50

[13] Mansuripur M 1990 *J. Appl. Phys.* **67** 6466–80

[14] Visnovsky S, Nyvlt M, Prosser V and Lopusnik Urban R 1995 *Phys. Rev.* B **52** 1090–106

[15] Oliver S A, DeMarzio C A, Lindberg S C, McKnight S W and Kale A B 1993 *Appl. Phys. Lett.* **63** 415–7

[16] Oliver S A, DeMarzio C A, Lindberg S C, McKnight S W and Kale A B 1994 *Opt. Eng.* **33** 3718–22

[17] Floraczek J M and Dan Dahlberg E 1990 *J. Appl. Phys.* **67** 7520–5

[18] Gao X, Glenn D W, Heckens S, Thompson D W and Woollam J A 1997 *J. Appl. Phys.* **82** 4525–31

[19] Balasubramanian K, Marathay A and Macleod H A 1988 *Thin Solid Films* **164** 391

[20] Schubert M, Tiwald T E and Woollam J A 1999 *Appl. Opt.* **38** 177–87

[21] Berreman D W 1972 *J. Opt. Soc. Am.* A **62** 502–10

[22] Yeh P 1980 *Surf. Sci.* **96** 41–53

[23] Lin-Chung P J and Teitler S 1984 *J. Opt. Soc. Am.* A **1** 703–5

[24] Zak J, Moog E R, Liu C and Bader S D 1990 *J. Magn. Magn. Mater.* **89** 107–23

[25] Gantmakher F R 1959 *Theory of Matrices* vol 1, transl K Hirsch (New York: Chelsea) ch 5

[26] Abdulhalim I, Benguigui L and Weil R 1985 *J. Physique* **46** 815–25

[27] Abdulhalim I, Weil R and Benguigui L 1986 *Liq. Cryst.* **1** 155–67

[28] Wohler H, Fritsch M, Haas G and Mlynski D A 1988 *J. Opt. Soc. Am.* A **5** 1554–7

[29] Abdulhalim I 1999 *J. Opt. A: Pure Appl. Opt.* **1** 646–53

[30] Yeh P 1988 *Optical Waves in Layered Media* (Toronto: Wiley) ch 6

[31] Winn J N, Fink Y, Fan S and Joanopoulos J D 1998 *Opt. Lett.* **23** 1573–5

[32] Fink Y, Winn J N, Fan S, Chen C, Michel J, Joanopoulos J D and Thomas E L 1998 *Science* **282** 1679–82

[33] Yablonovitch E 1998 *Opt. Lett.* **23** 1648–9

[34] Chigrin D N, Lavrinenko A V, Yarotsky D A and Gaponenko S V 1999 *Appl. Phys.* A **68** 25–8

[35] Chigrin D N, Lavrinenko A V, Yarotsky D A and Gaponenko S V 1999 *IEEE Trans. Micro. Theor. Tech.* submitted

[36] Abdulhalim I 2000 *Opt. Commun.* **174** 43–50